Occupant Safety in Highly Automated Vehicles – Challenges of Rotating Seats in Future Crash Scenarios

Julian Becker, Gian Antonio D'Addetta, Maja Wolkenstein, Freerk Bosma,
Ruud Verhoeve, Swen Schaub, Michael Sprenger, Michael Hamacher

Abstract This publication deals with the investigation of advanced occupant protection principles for rotated seating positions in highly and fully automated vehicles. In this context, a repositioning of the occupant into a safe seating configuration prior to a crash can be an integral part of a holistic safety concept.

The two presented principles address a passenger in a rotated position, pointing away from the driving direction. When a crash is imminent, the seat is rotated into the crash direction, to ensure airbag and seat-integrated three-point belt system can provide restraint. While in the first protection principle the seat is actively rotated, in the second principle the rotation is caused by the inertia of the seat and occupant. A Simcenter Madymo Active Human model in a generic multibody vehicle interior representation was used to investigate these principles, focusing on the effects of rotational repositioning on the occupant's kinematic response. Based on a simulation study, the responses on different parameter settings for the two principles were analysed. It is shown that the two repositioning mechanisms can bring the occupant closer to a standard position prior to a crash. Recommendations for corresponding timeframes as well as rotational axes for a full-frontal crash are given.

Keywords Active Human Body Model, Automated Driving, Occupant Safety, Seat Inertia, Seat Rotation.

I. INTRODUCTION

The EU Horizon 2020-funded OSCCAR project (Future Occupant Safety for Crashes in Cars) [1] is working on a novel simulation-based approach to safeguarding occupants in future vehicle accidents. Currently, there is no industry-wide standardisation for virtual testing that includes the advanced injury risk assessment using human body models (HBMs), which is required to allow virtual homologation and approval topics [2]. OSCCAR is working on providing an example homologation demonstration test case. For this development, standardised assessment of complex new accident scenarios and safety systems are proposed, including advanced and reliable simulation techniques. Even more so, the safety assessment traditionally done with anthropomorphic test devices, commonly known as crash test dummies, will need support from HBMs. These can cover new sitting postures and can represent the diversity of human beings. Safeguarding all types of occupants in new, comfortable seating positions and sitting postures will most likely be the crucial enabler for exploiting the promised overall safety benefit of highly automated vehicles (HAVs).

In the transition period from conventional to autonomous driving, new challenges for occupant safety will emerge. Within HAVs, passengers will benefit from an increased spatial freedom along with potential changes in interior and seating design [3]. Configurations with rotating seats may allow a higher degree of communication between passengers. These new rotated seating positions will, however, pose novel challenges for current restraint systems. The study investigates inward rotated seats prior to a frontal vehicle crash and focuses on the effects of turning seats back to a more beneficial situation before the crash takes place and interaction with the airbag commences. This mechanism is hereinafter referred to as protection principle (PP). The study includes initial occupant restraint analysis for current restraint systems, comparing the results for different seat rotation principles.

J. Becker (e-mail: julian.becker@ika.rwth-aachen.de; tel: +49 241 80 25641) is Research Assistant at Institute for Automotive Engineering (ika) - RWTH Aachen University. G. A. D'Addetta (Dr.-Ing.) is Team Leader and M. Wolkenstein is CAE Engineer at Robert Bosch GmbH. F. Bosma and R. Verhoeve are Senior Engineers at Siemens Industry Software and Service B.V. S. Schaub (Dr.-Ing.) is Senior Manager Engineering Strategy and M. Sprenger (Dr.-Ing.) is CAE Engineer at ZF Friedrichshafen AG. M. Hamacher (Dr.-Ing.) is Technical Leader Vehicle Safety and Vulnerable Road User Protection at fka GmbH.

Recent studies have investigated different seat rotation angles in combination with different impact directions. The main issues were observed when the seat was not facing in the direction of the crash. Physical test results have been presented in [4] [5] and [6] using a THOR-M and a Hybrid-III dummy to investigate the reproducibility and to assess the effects of seat rotation or different pulse directions. References [7] [8] and [9] presented results using human body models (HBMs) for similar investigations. All studies focused on interaction between occupant and belt system. Interactions with airbag systems and interior structures were mostly excluded. One finding was that for shoulder belts an inward seat rotation in frontal crash cases could lead to unfavourable belt to neck contact for high rotation angles, which showed increased Neck Injury Criteria (Nij) [6] and Neck Moment (M_y) [7] values. Apart from complex cervical spine loadings, neck to belt contact can cause a blunt carotid artery injury, which can lead to serious consequences for the patient [10].

In [4-9] possible seat-integrated countermeasures are discussed, to ensure safety under all potential rotation angles. Lateral seat support structures and headrest enlargement, as well as seat-integrated belt systems (see [5-6]), were introduced to restrain the occupant on a rotated seat in all impact directions. Active seat rotation is discussed in [8]. The effects of the rotation mechanism were investigated in [8] for a timeframe of 200 ms and for inward and outward initial rotation angles of +/-45° and +/-90°, leading to average rotation velocities of 45°/200 ms (equals 225°/s) and 90°/200 ms (equals 450°/s). It was found that higher angular rotation velocities led to higher injury risks already during the pre-crash phase. This applies for the Brain Injury Criteria, Nij, chest deflection, possible rib fractures and for the C2-C7 ligament strains. Following [8], rotations of 45° within 200 ms seem feasible. For 90° rotations within 200 ms, some ligament strains, in particular, are above the injury threshold.

The reviewed literature sources showed possible safety deficiencies in rotated seating positions. Several countermeasures were already discussed in recent studies. When it comes to active countermeasures, like a rotation of the seat and the occupant prior to a crash into a more beneficial position, available literature is limited. With respect to a lack of validated occupant models for pure rotational loading conditions, these scenarios need to be further investigated. This study aims to give an insight into the occupant's kinematic behaviour for two rotational based safety measures.

II. METHODS

Simulation Model and Crash Case

The generic multibody interior model that was created for OSCCAR to study potential PPs has its origin in the "Simcenter Madymo Active Human Model (AHM) Integrated Safety Application" version 3.0 [11]. The presented generic multibody interior model is aligned with the LS-Dyna model, as described in [12], and contains state-of-the-art restraint systems, a seat (see Appendix) and a passenger (see Figure 1), which is represented with the Simcenter Madymo AHM v3.1. Figure 1 also illustrates the acceleration-based motion that is used in the presented study, a 1 g automated emergency braking (AEB) manoeuvre followed by a crash (US NCAP Full Width Rigid Wall 56 km/h crash pulse). The Simcenter Madymo AHM which is used in this study is validated for frontal, lateral (combined frontal, lateral), rear and vertical loading conditions. The intervertebral discs of the neck and spine are modelled by point restraints and cardan restraints, based on stiffness data from literature (see [13] for more information on the model validation).

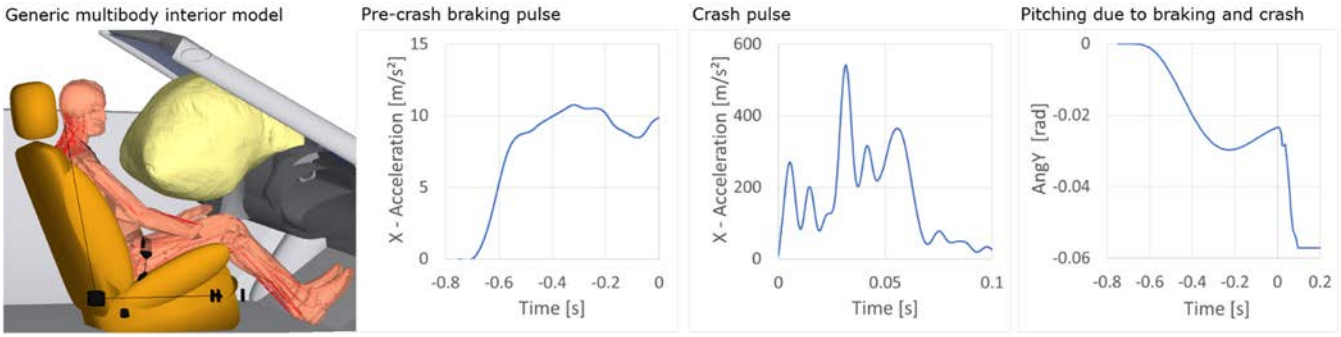

Fig. 1. Generic Simcenter Madymo multibody interior model and pulses.

Since the generic multibody interior model is a combination of several generic (safety) components [11-12], it was considered important that all these generic components work well together and deliver plausible results. Therefore, an initial simulation performance check of the generic multibody interior model was performed using a Hybrid-III 50th and a Hybrid-III 5th percentile Simcenter Madymo dummy (d_hyb350el_Q version 2.0 2017-04-12 R7.7 and d_hyb305el_Q version 2.0 2017-05-18 R7.7) against the generic 56 km/h rigid barrier crash pulse for both the driver and passenger, respectively. The injury peak values of the Hybrid-III dummy models were recorded and, in order to have a qualitative indication of the model performance, the rating scheme of US NCAP [14] was used to rate the simulation results. In these simulations, both driver and passenger scored a four-star rating.

The generic multibody interior model is highly parameterised in order to study parameter variation effects in a design of experiment (DoE) study or optimisation. For the DoE studies of the two PPs, two different software tools were used, therefore the colour plots of the response surface are not always aligned in this paper. The most relevant chosen settings of enabled features in the model as used in the presented study are shown in Table I; additional model settings can be found in the Appendix in Figure A1.

TABLE I
MAIN GENERIC MODEL SETTINGS

Description	Unit	Protection Principle 1	Protection Principle 2
Simulation start time	ms	[-750; (…); -150]	-750
Simulation end time	ms	180	180
Activation time	ms	[-400; (…); -50]	-750
AEB activated	-	Yes; No	Yes
Belt in seat	-	Yes	Yes
Retractor Load Limiter	N	2700	2700
Buckle pretensioner firing time	ms	10	10
Buckle pretension Force	N	2000	2000
Passenger airbag	-	Generic	Generic
Passenger airbag firing time	ms	10	10
Initial seat rotation angle	°	[0; (…); 30]	30

Protection Principle 1 (PP1)

The overall motivation for the first protection principle (PP1) is to ensure occupant safety in rotating seats (rotation around z-axis, see Figure 2 (left)). Therefore, the occupant on a rotated seat is repositioned into a close to standard frontal facing position prior to a vehicle crash. The rotation curve is characterised by a spline interpolation (see Figure 2 (right)). Thus, a plausible kinematic behaviour of the seat without jerk motion is appearing. For the analysed cases, it was assumed that in a frontal facing position, the occupant is optimally restrained. Initially the occupant is sitting slightly rotated and pointing away from the driving direction.

The analysed scenario represents a highway pilot driving situation with an occupant sitting on the passenger seat. Automatic braking may occur before the collision, possible steering manoeuvres are not considered in this study. The initial situation includes a seat rotation of up to 30°. As key simulation variables, the rotation velocity and the starting time of pre-crash rotation are varied. In each case the pre-crash rotation action terminates at T = 0 ms (time of collision). Table I summarises the boundary conditions.

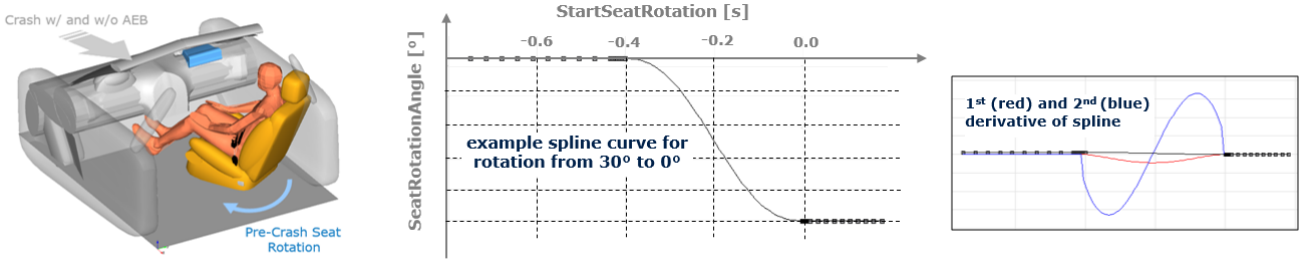

Fig. 2. Scheme of PP1 (left) and one example for the seat rotation curves (right).

The simulation assessment was carried out via the known HBM kinematic values. To assess the pre-crash phase and the effectiveness of the seat rotation in detail, relative measures between the seat and HBM body parts are considered, defined as relative head angle β1, relative shoulder angle β2, relative pelvis angle β3 and relative knee angle β4 (see Figure 3 (left)). A crucial effect during the rotation of the seated occupant is the seat belt to neck interaction. To facilitate the analysis, a measuring "tool" was included into the HBM's neck. A spherical ellipsoid surface (shown in green in Figure 3 (right)) was attached to the C7 body of the neck and an additional contact with negligible contact stiffness between shoulder belt and ellipsoid was introduced. The ellipsoid surface is completely inside the outer element surface of the HBM neck and therefore does not produce any HBM surface change. The ellipsoid surface only enables measurement of the local penetration of the belt into the neck surface, which is allowed by the force-penetration contact definition.

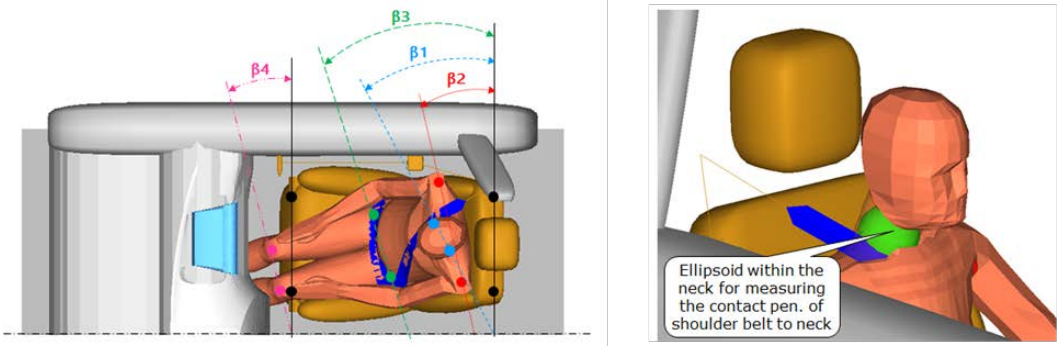

Fig. 3. Definition of relative angles between occupant and seat (left), additional ellipsoid surface for evaluation of belt to neck contact.

Protection Principle 2 (PP2)

Protection principle 2 (PP2) describes a special case of PP1. In contrast to PP1, the rotation of the seat and the occupant seated on it is caused solely by the mass inertia of the system (seat and occupant). The automated emergency braking (AEB) prior to the crash initiates the relative acceleration of the masses required to rotate the seat. This makes the PP2 a "passive" protection principle, which only works when AEB is applied.

In the PP2 study, the seat is initially rotated by 30° to the centre of the vehicle. To allow the seat to rotate freely, a revolution joint, connecting the seat to the vehicle, is released at -750 ms time to collision, when the emergency braking is applied. The joint is locked as soon as the seat reaches an angle of 0° (standard seat rotation angle in a forward-facing position). In the simulation study the seat rotation was performed with different rotational axes, varying from min. to max. x- and y-coordinates, as shown in Figure 4. In addition to the position of the rotational axis, the position of the centres of gravity (COG) of the seat and the occupant are also shown in Figure 4. Whereas the COG of the seat is fixed relative to the seat, the COG of the occupant depends on the occupant's movement during the event. The effect of the belt pre-tensioner on the occupant's movement was not investigated in this study. The pre-tensioner firing time and force was kept constant as shown in Table I.

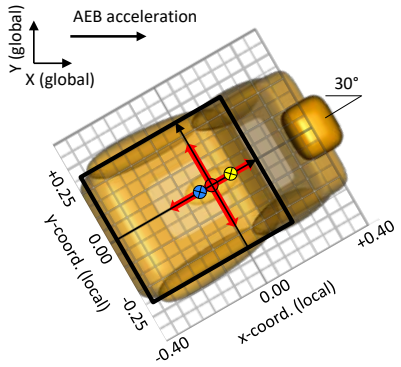

Parameter Setting	Unit	Value
Initial seat angle	°	30
Locking seat angle	°	0
Min. x-coord. of rotation axis	m	-0.37
Max. x-coord. of rotation axis	m	0.18
Min. y-coord. of rotation axis	m	-0.25
Max. y-coord. of rotation axis	m	0.25

Fig. 4. Seat model in the initial position, including the local coordinate system of the seat centred in the H-Point. COG of the occupant (blue), COG of the seat system (yellow), rotation axis (red).

III. RESULTS

Protection Principle 1 (PP1)

The DoE simulation study was defined according to the conditions listed in Table I, with 1° to 30° as initial seat rotation and with pre-crash seat rotation ending at T = 0 ms. A variation of seat-base angle (around z-axis) and the start time of the seat rotation in the pre-crash phase creates a response surface for the relative β-angles, as shown in Figure 5. The black dots represent the corresponding simulation conditions, while the colouring defines the difference angle from 0° to -20°. White coloured areas within the diagram represent values above the upper limit, grey areas represent values below the lower limit. The upper part of the figure represents a situation in which no AEB is applied, while the lower part shows the results where the braking action is included. The effect of the protection principle on the occupant position relative to the seat is investigated at the time of the crash (T = 0 ms) and at T = 35 ms, just before the occupant contacts the passenger airbag.

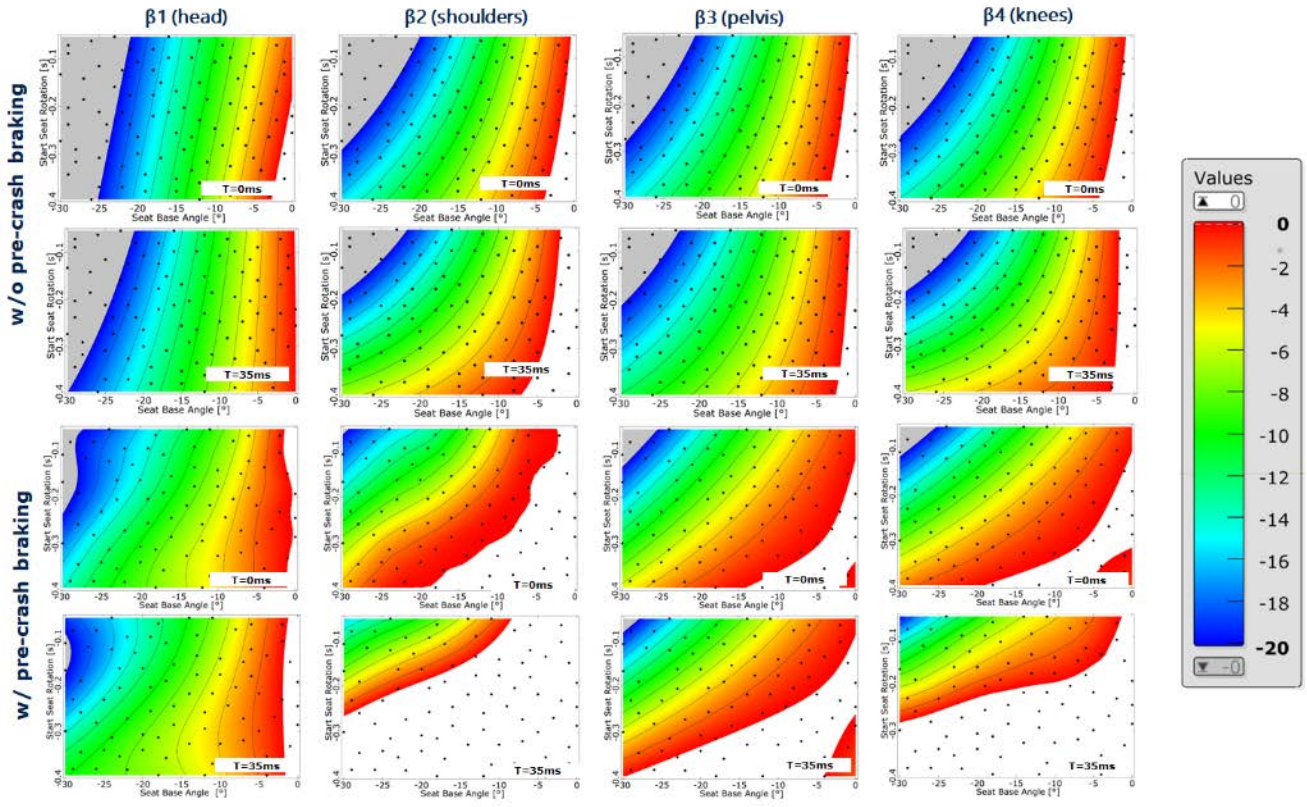

Fig. 5. Relative occupant to seat rotation angles [°] (head angle β1, shoulder angle β2, pelvis angle β3, knees angle β4). Without AEB (top) and with AEB (bottom). X-axis represents the initial seat-base rotation angle [°] from -30° to 0°. Y-axis represents the start time of seat rotation [s] from -0.4 s to -0.05 s.

The pre-crash braking has a favourable effect on the occupant repositioning, i.e. the values are lower in this case (red colour) and thus the occupant follows the seat rotation more closely than without braking. In cases with a high relative angle (blue), the occupant follows the seat rotation with delay, i.e. the faster the seat rotation, the more delayed the occupant movement. Typically, a pre-crash braking induces an occupant forward movement out of the seat, hence reducing the contact to the seat. Nevertheless, in these cases the contact with the belt system will significantly be improved and the occupant is coupled in a more robust manner to the seat rotation. Thus the occupant follows the seat rotation in a more favourable way. Apparently, the relative head angle β1 shows less influence of the rotation compared to the other angles, even for lower rotation velocities (see also Appendix, Table AI for chosen model settings). This means that the head movement is delayed with respect to the rest of the body and therefore shows higher relative angles. The occupant position and posture just before the first contact with the airbag is considered as important as at the start of the crash (T = 0 ms). Thus, an additional analysis for T = 35 ms is included in Figure 5. Further alignment between seat and occupant movement is seen, particularly with pre-crash braking.

The analysis of occupant body accelerations in the pre-crash phase gives further indication of the kinematics. The pre-crash braking yields higher overall resultant accelerations compared to a situation without any braking (see grey areas in Figure 6). Without braking, only the effect of the seat rotation is seen. However, the resultant accelerations are on a low level overall and reach values of up to 6 g for the fastest seat rotation.

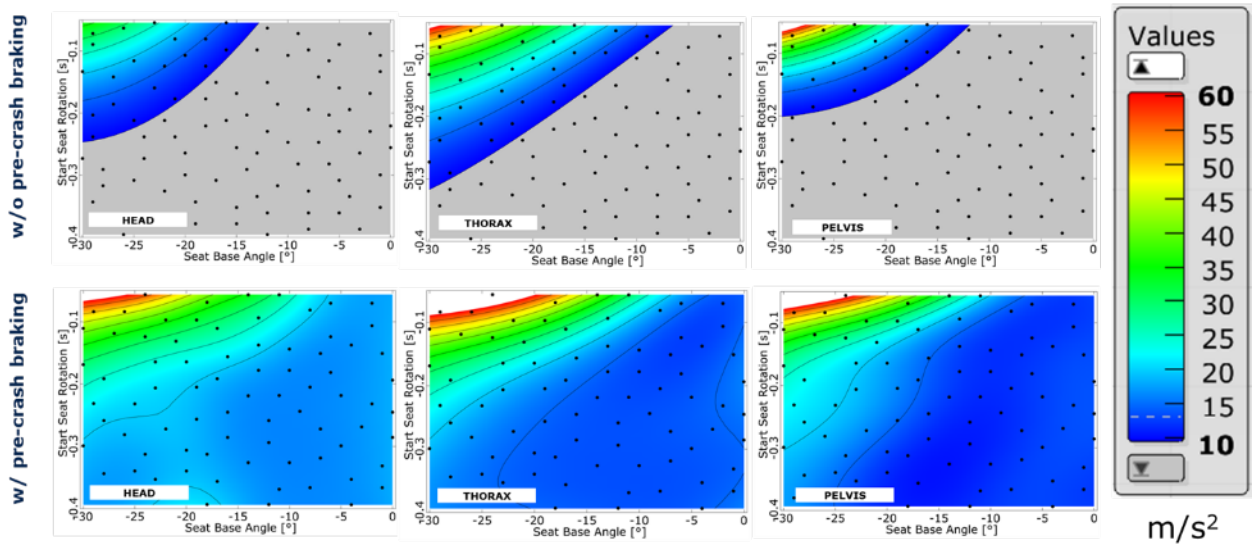

Fig. 6. Pre-crash resultant acceleration [m/s²] of head, thorax and pelvis without AEB (top) and with AEB (bottom).

In a second simulation series the seat rotation velocity was kept constant, but the starting time was varied. Thus, situations arose where the seat rotation was completed before the crash began, e.g. for case m400 starting at –400 ms and ending –200 ms before the crash starts. The rotation duration for 30° was fixed to 200 ms (equals 150°/s) and the starting time varied from -400 ms to -200 ms. Only cases without pre-crash braking were analysed. The focus was on kinematic values, like relative angles βi, and resultant accelerations. The relative angles βi were measured at T = 0 ms and compared with the maximum values during the pre-crash phase. Figure 7 shows that the maximum relative angles are independent of the starting time of the rotation. With the chosen rotation velocity of 150°/s, a rather large angular difference between occupant and seat may appear during the pre-crash action. Occupant inertial effects have a beneficial impact on the relative angle at T = 0 ms, even if the rotation was stopped 200 ms before the crash. The relative angles at start of crash at T = 0 ms scale with the starting time of the rotation.

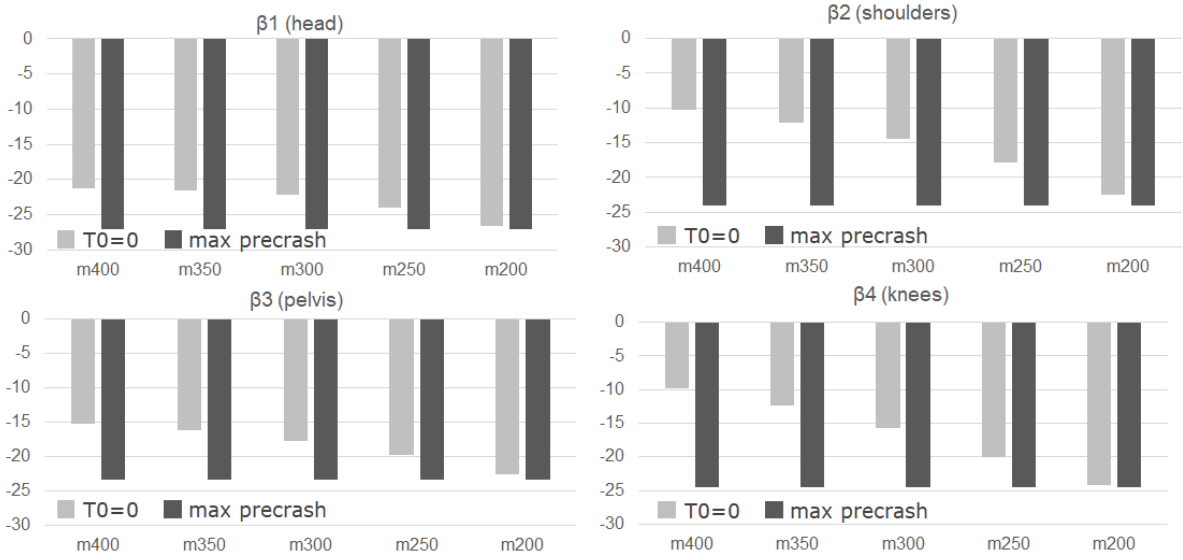

Fig. 7. Relative occupant to seat rotation angles [°] (head angle β1, shoulder angle β2, pelvis angle β3, knee angle β4). Maximal angle during pre-crash phase (dark grey) and angle at T = 0 ms (light grey).

The later the rotation starts the higher the absolute relative angle values at T = 0 ms and the less time the occupant has to reach the final direction of 0°, facing fully forward. This effect is also seen in the βi vs. time diagram in Figure 8. Relative angles for shoulder and knee are affected more strongly by the inertial effect than those for the pelvis and head. The results show that the chosen rotation velocity is rather high, and one can expect lower effects and better occupant guidance for lower rotation velocities.

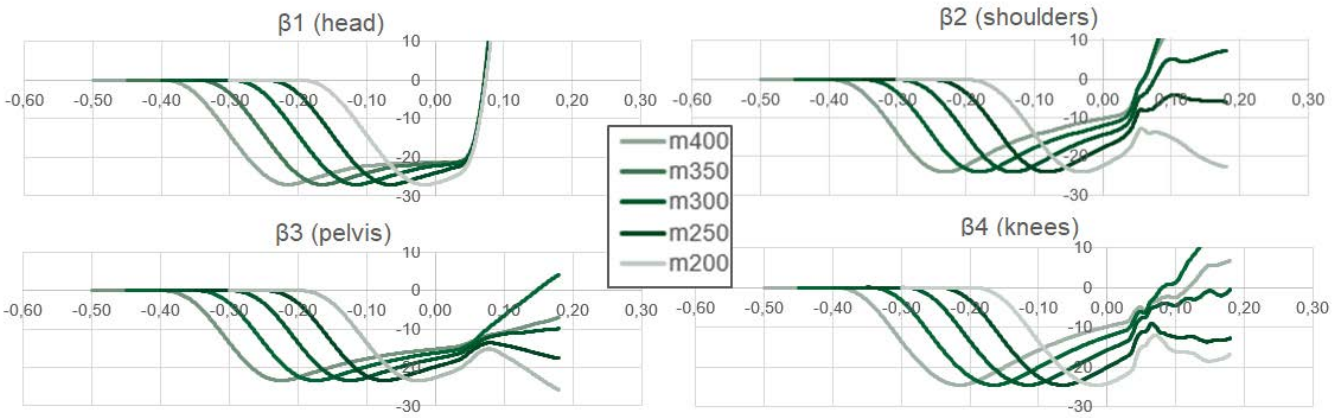

Fig. 8. Relative occupant to seat rotation angles [°] (head angle β1, shoulder angle β2, pelvis angle β3, knee angle β4) vs. time [s].

As the evaluation of the body accelerations in the pre-crash phase in Figure 9 (top) illustrates, the maximum accelerations are overall at a very low level and show no significant correlation. Accelerations in the crash phase in Figure 9 (low) also do not show any distinctive features and may indicate that the starting point of the seat rotation action (for the given high velocity) has a low impact on the occupant body load.

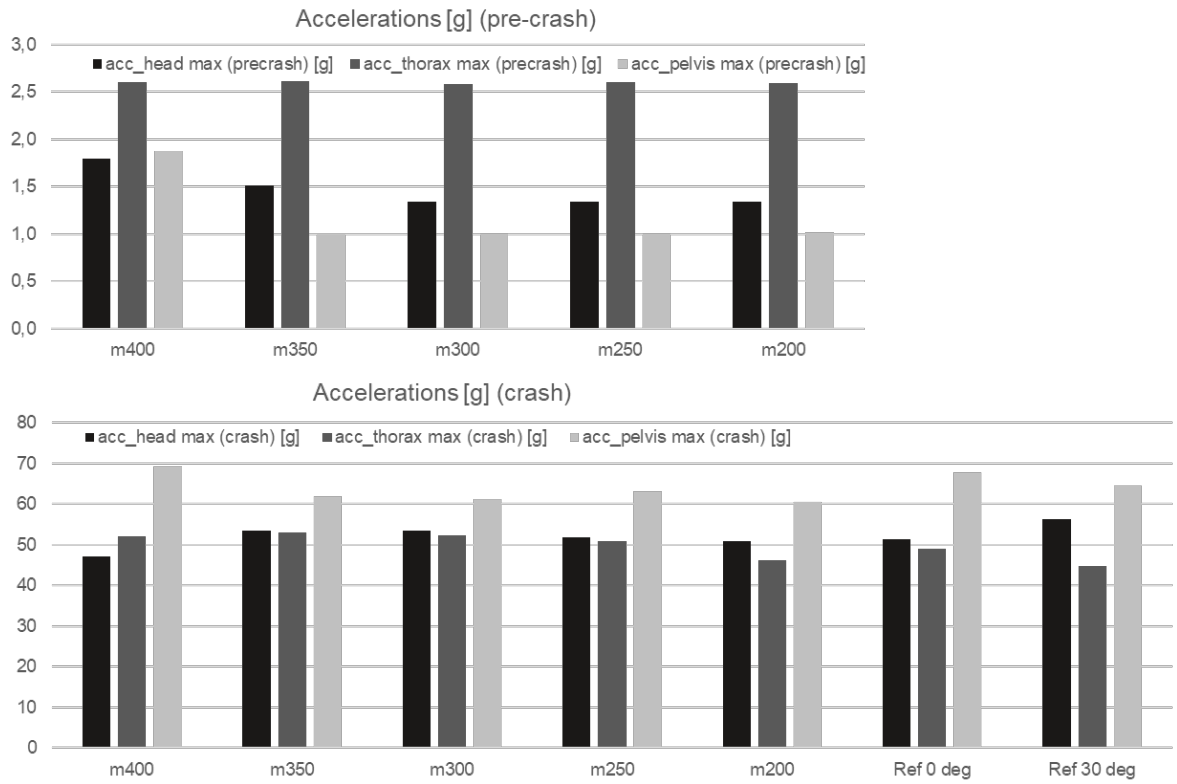

Fig. 9. Head, thorax and pelvis acceleration [g] for pre-crash and in-crash phases with different rotation start times.

As pointed out in the Methods section, a crucial effect during rotation of the occupant is the belt to neck interaction. A kinematic injury risk indicator was proposed (see Figure 3 (right)). The DoE was evaluated accordingly with and without pre-crash braking. The results of the neck injury indicator are shown in Figure 10. No contact is visible in any case during the pre-crash phase. The picture changes in the crash phase. Without pre-crash braking, no contact is visible between 0° and 13°, while with a braking action this region is between 0° and 7°. As result, no pre-crash seat rotation would be needed in the defined angle regions from the point of view of the neck injury predictor. In comparison, the overall belt to neck contact is lower, particularly for higher initial seat rotation angles (> 20°), for cases with pre-crash braking compared to those without. It is presumed that pre-crash braking allows for a better coupling of the occupant to the vehicle in the crash situation.

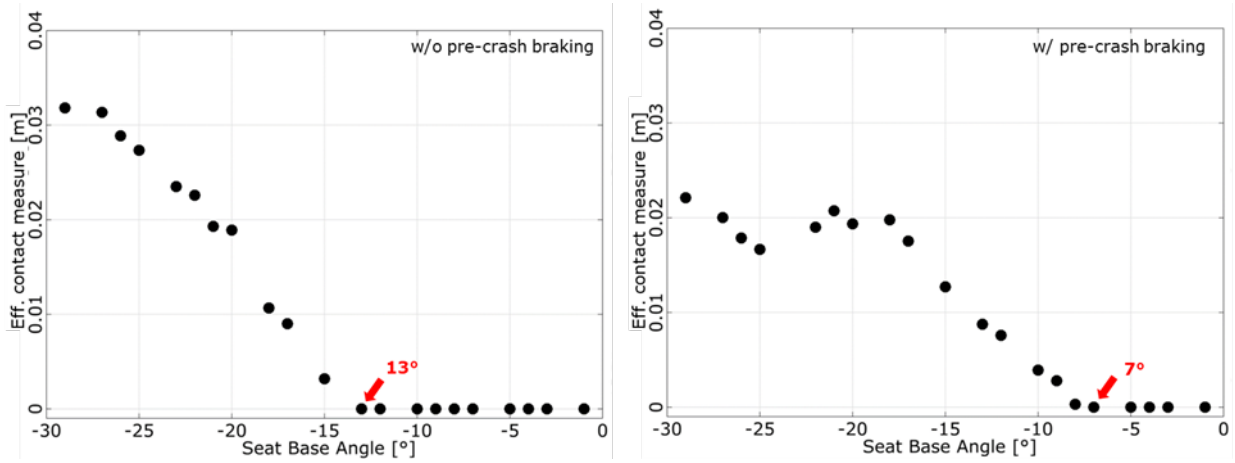

Fig. 10. In-crash belt to neck contact [m] without AEB (left) and with AEB (right).

The evaluation of the complete field with a pre-crash seat rotation characteristic is shown in Figure 11. As explained, the pre-crash seat rotation start time varied from T = -400 ms to T = -50 ms and ends at T = 0 ms. With increasing rotational velocity, increasing neck contact is observed. As in Figure 10, the contact is measured in fractions of meter. Similar to the case with static initial seat rotations, no contact is visible during the pre-crash phase and the braking action has a favourable effect on the contact, e.g. lower absolute values of contact and a broader region with negligible contact (seen in blue) in Figure 11, right.

The effect of higher shoulder belt to neck contact with increasing rotation velocities is envisioned, for example, by comparing simulation SIM43 (slow seat rotation) to SIM78 (fast seat rotation) (see Figure 12, left). If a function to minimise seat belt to neck penetration were desired, the white dotted line on the right-hand side of Figure 12 could represent an adequate approach. For smaller initial rotations, higher rotational velocities are acceptable.

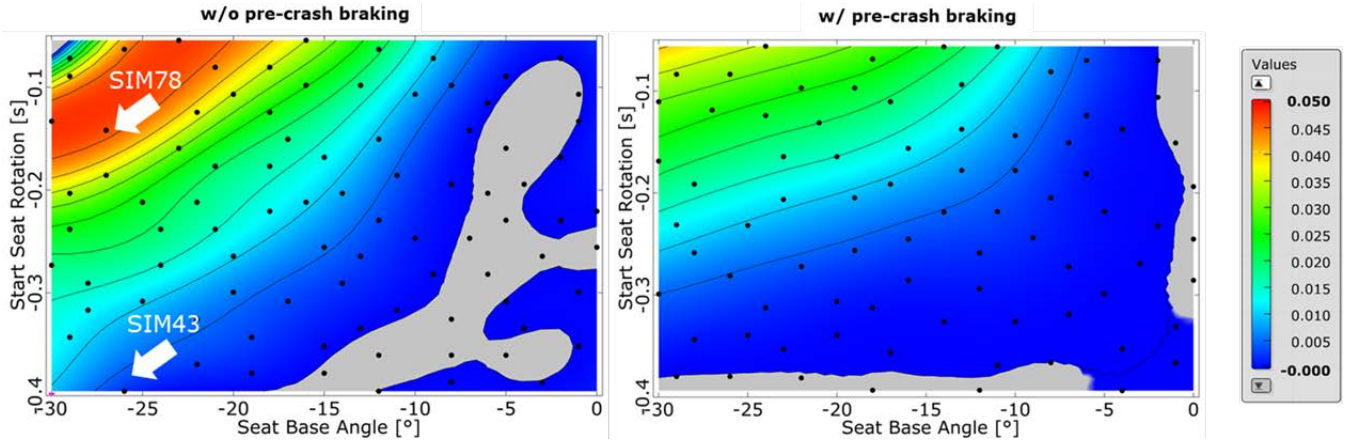

Fig. 11. In-crash belt to neck contact [m] as function of initial seat-base angle [°] and seat rotation start time [s]. Without AEB (left) and with AEB (right). Grey colour represents value 0 (negative values caused by response surface smoothing method).

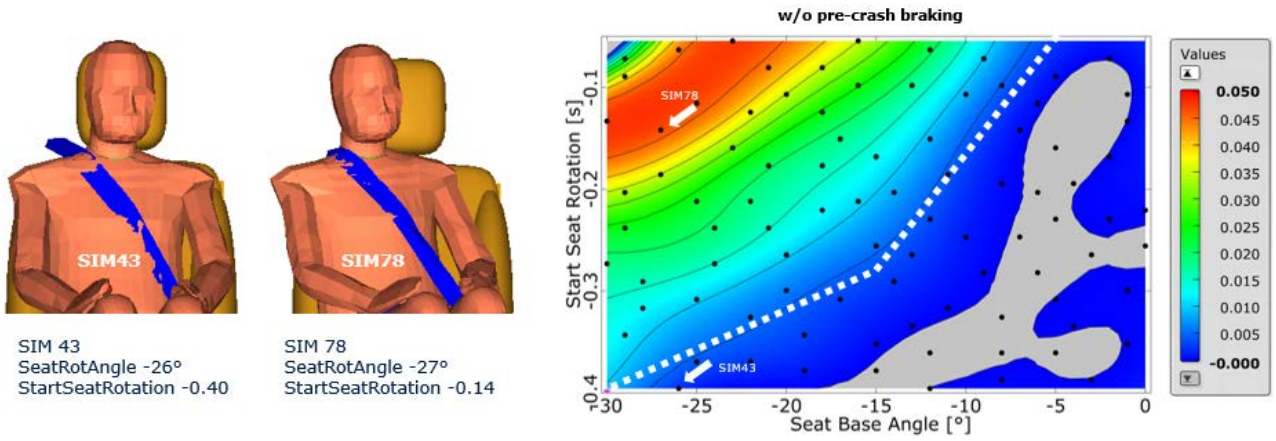

Fig. 12. Comparison of shoulder-belt position for two different average rotation velocities (SIM43 (65°/s) and SIM78 (193°/s)) without AEB at T = 5 ms (left). Function for seat rotation based on in-crash belt to neck contact evaluation (white dotted line) (right).

Considering simulation studies with static and dynamic seat rotations, i.e. the seat is not rotated back to the 0° position but to that in Fig. 10 (0° to 7°/13°), a later start of the pre-crash rotation with a rotation velocity as defined by the white dotted line of Fig. 12 is feasible. In the case of SIM43, for example, the rotation velocity is 65°/s. If the occupant needs only to be rotated from -26° to -13° and the same rotation velocity of 65°/s is applied, the rotation action can be started 200 ms before crash instead of 400 ms. This would allow for a later detection and less ambitious requirements for the pre-crash detection system.

Protection Principle 2 (PP2)

A simulation study according to the definition given in Fig. 4 was conducted for PP2. Different rotation behaviours of the seat system were generated by varying the x- and y-coordinates of the rotation axis. Based on the simulations, a response surface was created for the time at which the seat reached a rotation angle of 0° (locking-time) (see Fig. 13).

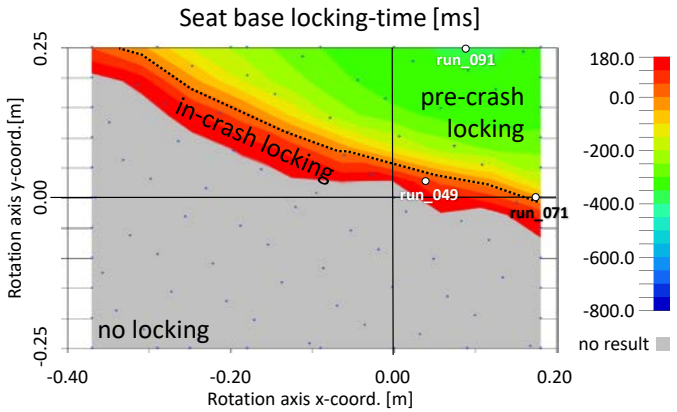

Fig. 13. Response surface of the seat locking-time [ms] for different positions of the rotation axis positions.

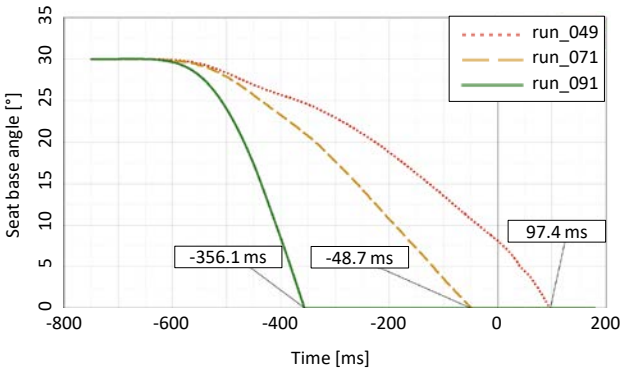

Fig. 14. Seat rotation angle [°] vs. simulation time [ms] for simulation run_049, run_071 and run_091.

The response surface can be divided into three locking-time areas: “pre-crash locking”, where the locking angle is reached before the crash (-750 ms < locking-time < 0 ms); “in-crash locking”, where the locking angle is reached after the crash starts (0 < locking-time < 180 ms); and “no locking”, where the locking angle of the mechanism is not reached during the simulated timeframe. The boundary between pre-crash and in-crash locking is illustrated as dotted line in Figure 13. The limit between in-crash and no locking defines the feasibility of the principle (boundary between red and grey coloured boundary). Rotational axes positioned within the grey-coloured area cause the seat to rotate in the opposite direction such that the locking angle is not reached and the feasibility of the principle is not given. In general, Figure 13 shows, for the feasible cases, that with larger global Y-distance

between the system COG and the rotational axis (leverage to induce the rotation torque), early locking times are reached and therefore the highest average rotation velocities are generated. In cases where the locking angle is reached, three simulation runs (run_049 (x = 0.04, y = 0.02), run_071 (x = 0.18, y = 0.00), run_091 (x = 0.09, y = 0.25)) are shown for illustration in Figure 14. Whereas run_049 is the simulation with the latest locking-time (at T = 97.4 ms), run_071 describes the simulation with the latest locking-time within the pre-crash phase (at T = -47.7 ms) and run_091 shows the earliest locking-time of all performed simulations (at T = -356.1 ms).

The relative position of the occupant to the seat is shown in Figure 15 at T = 0 ms and T = 35 ms for different rotational axis positions. The response surfaces of the β-angles were created only from the cases where the principle was feasible. The later the locking-time is reached, the higher the relative angles between occupant and seat, while the head (β1) shows the highest relative angles, especially during early locking times. The lowest relative angles are obtained for the knee (β4) as well as for the shoulder (β2). Overall, it can be concluded that the more time the occupant has to follow the seat's movement, the smaller the angles between the seat and the occupant. Apart from that, there were no significant differences observed in the β-angles for T = 0 ms and T = 35 ms, which shows that the occupant's position changes only marginally until contact with the airbag.

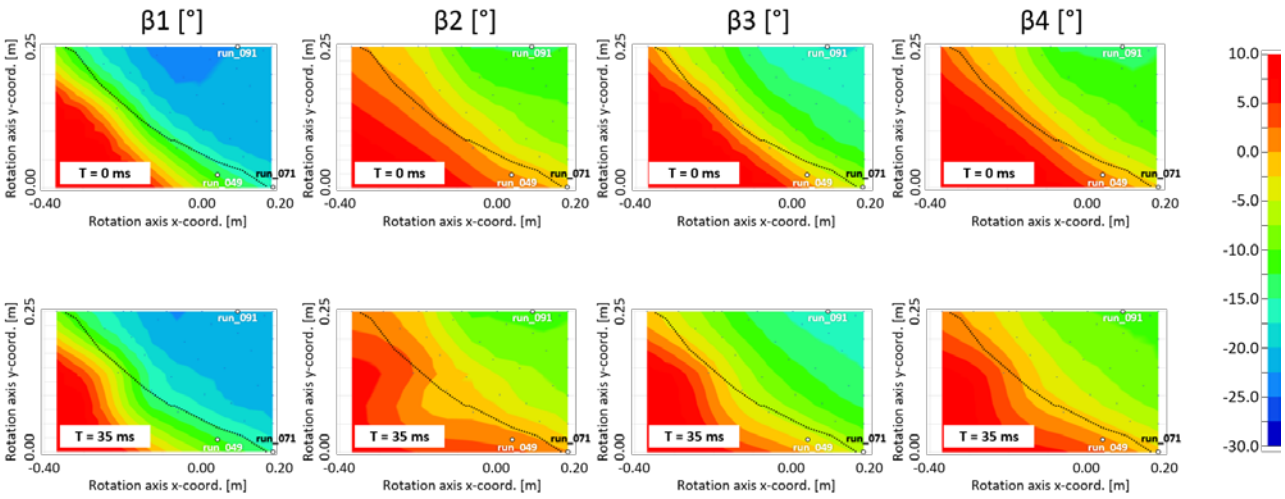

Fig. 15. Relative occupant to seat rotation angles [°] (head angle β1, shoulder angle β2, pelvis angle β3, knee angle β4) for various rotation axis positions [m]. Boundary between pre- and in-crash locking-time (dotted line).

These observations, based on the response surfaces of the relative angles, can also be seen in the numerical values of the example simulation runs (see Figure 16). The highest relative angle of the head of the occupant also appears in this comparison. In contrast to the head angle (β1), a significant reduction for the knee (β4), shoulder (β2) and pelvis angles (β3) can be achieved through a reduced seat rotation velocity.

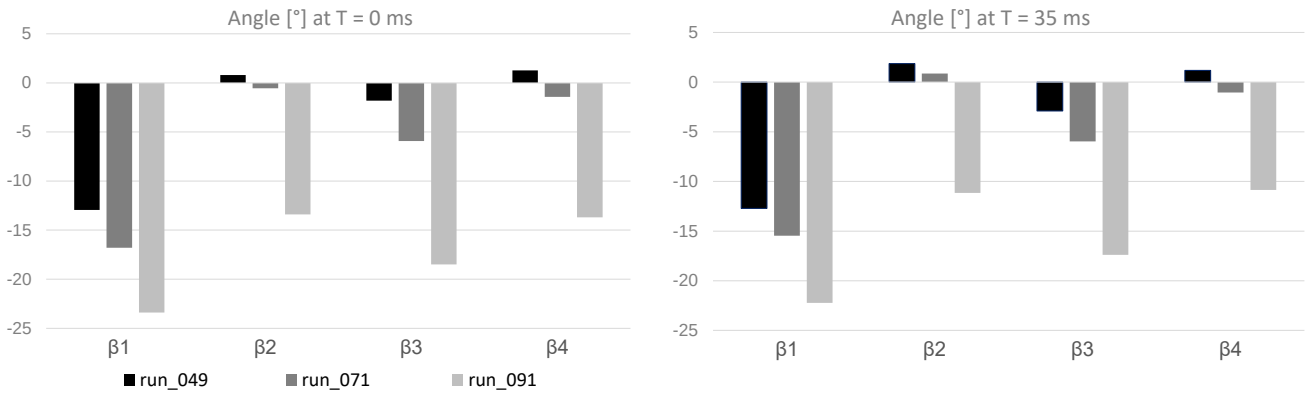

Fig. 16. Relative occupant to seat rotation angles [°] (head angle β1, shoulder angle β2, pelvis angle β3, knee angle β4) for exemplary simulation runs at T = 0 ms (left) and T = 35 ms (right).

The PP2 results show that the principle can be feasible under certain conditions. For a situation where AEB (without steering) is applied and the passenger seat is initially rotated up to 30°, a first limitation of feasible positions of rotational axis was observed. With a variation of the rotational axis position within the limited range, different locking-times can be reached. The locking-time can give an insight into the application range of the principle, defining how much time is necessary to reach a locking. Due to inertia effects the locking of the system does not mean that the occupant was fully repositioned to a standard seating position. Even if the seat has already reached the final position, the occupants movement is delayed, which was shown with the β-angles. On the one hand it can be observed that the delay between occupant and seat is lower the later the locking time. On the other hand late locking can cause an over rotating of the occupant. Due to the delayed occupant movement also a sudden locking of the seat is not generating jerk motions of the AHM.

Comparison of PP1 and PP2

In the following section, the effects of the two reposition mechanisms of PP1 (active, motorised) and PP2 (passive, inertia-based) on the AHM position at time T = 0 ms and T = 35 ms are compared. The simulations run_071 and run_091 of PP2 were considered as exemplary cases. To ensure comparability of the results, the same axes of rotation and locking-times were chosen for PP1 as in the two PP2 simulations. For PP1 a rotation speed was chosen that corresponds to the largest slope of the PP2 rotation curves. Therefore, an average rotation velocity of 60°/s was selected for run_071 and 200°/s for run_091 (see Table II). The relative angles for PP1 and PP2 are shown in Figure 17. Corresponding images from the simulations can be found in the Appendix in Table AII.

TABLE II
DEFINITION OF COMPARED SIMULATION RUNS

Simulation run	x-coord. rotation axis [m]	y-coord. rotation axis [m]	Average rotation velocity [°/s]
PP1 run_071	0.18	0.00	60
PP1 run_091	0.09	0.25	200
PP2 run_071	0.18	0.00	43
PP2 run_091	0.09	0.25	76

For run_071 (PP2 simulation with the latest locking-time in the pre-crash time), PP1 leads to higher relative repositioning of the occupant compared to PP2. In comparison to PP2, this leads to lower relative angles between the occupant and the seat for β1 (head) and β3 (pelvis), whereas for β4 (knees) and β2 (shoulders) the higher relative rotation even leads to the occupant over-rotating. In run_091 (PP2 simulation with the earliest locking-time), it was observed that the repositioning of the occupant to T = 0 ms was lower for PP1 compared to PP2. Nevertheless, at T = 35 ms the relative angles β1 (head) and β2 (shoulders) of PP1 are closer to the standard position than the angles of the PP2 simulations. Therefore, when applying PP1, the occupant has a higher rotational movement in the 35 ms timeframe until contact with the airbag, which leads to a more centralised position of the upper body relative to the seat (β-angles closer to zero) compared to PP2.

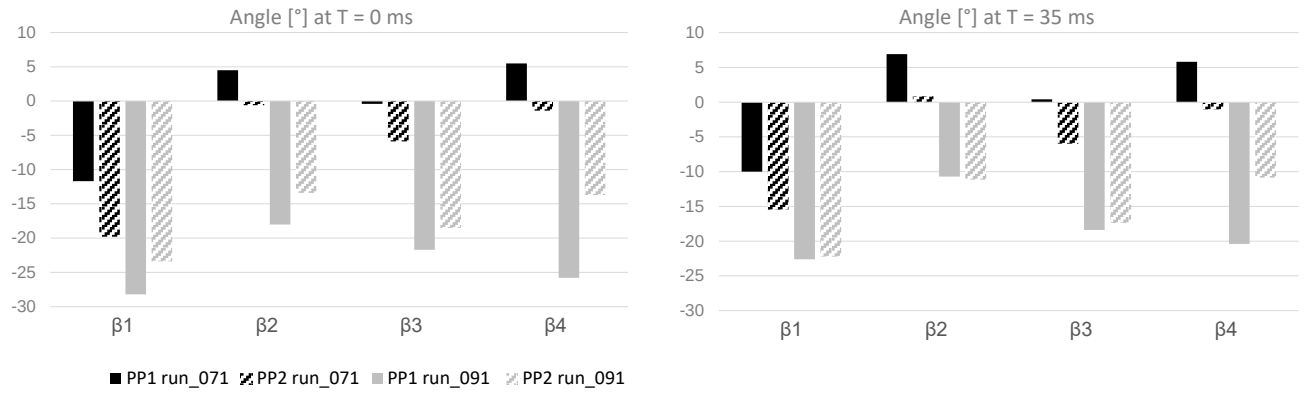

Fig. 17. Relative occupant to seat rotation angles [°] (head angle β1, shoulder angle β2, pelvis angle β3, knee angle β4) for exemplary simulation runs of PP1 and PP2 at T = 0 ms (left) and T = 35 ms (right).

IV. DISCUSSION

The Simcenter Madymo AHM was subjected to novel loading conditions, including an initially rotated seating position and a seat rotation phase prior to crash, with and without pre-crash braking. Initial analyses concerning the assessment of the HBM loading were drafted. Furthermore, new generic protection principles to reposition the occupant from a rotated seat position were investigated. PP1 and PP2 are very similar in their working principle. PP2 can be considered as a special case of PP1 as the torque which is required to reposition the seat in is not provided by an actuator, but arises intrinsically from the inertia of the seat and occupant on a correctly positioned pivot.

To investigate the effectiveness of rotating the seat into the nominal position, four relative angles (β1 … β4) are defined, describing the angular difference between the seat orientation and the orientation of the occupant's knees, head, shoulder and pelvis, respectively. These relative angles can be used to describe the effect of the rotation principles as they indicate how well the different occupant regions can follow the seat rotation. A belt to neck contact interaction indicator is defined via a spherical surface attached to the occupant's neck, to identify unfavourable contacts between neck and seatbelt.

The observed occupant rotational behaviour in the AHM simulations looks natural and realistic (see Table AII in the Appendix). However, more parametric studies are needed to better understand the dependency on physical parameters, e.g. friction values, foam stiffness, etc. Furthermore, validation data would be needed to validate the occupant rotation quantitatively. Injury limit values for (A)HBM need further investigation, especially for investigating the risk of injury due to pre-crash occupant repositioning. State-of-the-art models and the analysis tools that come with them are still limited here and are lacking in available validation data. This needs to be considered when assessing the results presented in this study. Since (volunteer) rotational validation data is currently not available a comparison to other HBMs like Thums or GHBMC could provide additional information on the occupant behaviour under the applied rotational movement and can contribute to the question in which boundaries the protection principles can be safely applied.

Since the presented study required many simulations in a relative short amount of time the Simcenter Madymo AHM was chosen to achieve this. In total 350 simulations were performed with an average runtime of 1 hour per simulation with one CPU. The results from this study will be used as input for further investigations with Thums.

Comparing the two protection principles, PP1 performed better at achieving desirable occupant rotation, when starting time for the rotation is early enough and rotation speed is not too high. Pre-crash braking in general supports this principle due to better contact between occupant and seat belt. PP2 can also reach similar results for some pivot positions. However, the result is strongly dependent on the selection of the pivot position and the relative acceleration level before crash (pre-crash braking). Also the angle of the crash is expected to have an influence on the functionality of PP2, especially when the locking of the system is not reached prior to the vehicle impact. The effects of angled vehicle crashes on PP1 and PP2 were not investigated in this study.

The studies for both principles demonstrated that the occupant does not stop when the seat rotation stops, i.e. occupant rotation continues until contact to the airbag occurs. Therefore, the first point of occupant to airbag contact should be considered when assessing the effects of PP1 and PP2 on the final occupant loading during crash. A typical time of T = 35 ms was used for the load cases investigated here.

The performed simulation studies demonstrate how (A)HBMs can be used to investigate the described protection principles. The simulations show good capabilities qualitatively comparing different protection principles. For detailed studies or parameter optimisation, the validation status of the models and the lack of injury limit values define the application range.

V. CONCLUSIONS

It was shown that the two repositioning mechanisms can bring the occupant closer to a standard position prior to a crash. Based on the Simcenter Madymo AHM response, recommendations for corresponding timeframes as well as rotational axes for a full-frontal crash are given.

The relative movement of the occupant to the seat is a measurement of how well the occupant is repositioned and follows the seat movement. AEB improves the connection between the occupant and the seat belt, i.e. the relative angle between the seat and the occupant body parts (head, shoulder, pelvis, knees) are closer to zero. The higher the rotation velocity of the seat, the lower the guidance of the occupant to the seat, i.e. high relative

angles occur. Therefore, a timely rotation in the pre-crash phase is beneficial with respect to the relative position of the occupant to the seat at the beginning of the in-crash phase. In general, the acceleration of the occupant due to a repositioning in the pre-crash phase is lower compared to the maximum accelerations in the in-crash phase.

Within the crash, no belt to neck contact is detected for initial seat rotation angles < 7° and < 13° with and without AEB, respectively. Beyond these values the neck belt contact is lower when AEB is applied, especially for seat rotation angles > 20°. Lower rotation velocities lead to lower belt to neck contact.

The functionality of PP2 depends on the rotation axis, the seat angle, the system's centre of gravity and the acceleration direction. In general, PP2 shows a lower relative repositioning of the occupant between time T = 0 ms and T = 35 ms compared to PP1.

It must be noted that the results presented in this paper are intermediate results based on pre-studies. Further simulation studies with the described protection principles and other protections principles are currently underway in OSCCAR.

VI. ACKNOWLEDGEMENTS

The work described was carried out within the EU H2020 project "OSCCAR - Future Occupant Safety for Crashes in Cars". OSCCAR has received funding from the European Union's Horizon 2020 research and innovation programme under grant agreement No. 768947.

VII. REFERENCES

[1] OSCCAR Project. "OSCCAR project website," Internet: [http://www.osccarproject.eu/], [27 March 2020].

[2] Eggers A, Mayer C and Peldschuss S. Validation procedure for simulation models in a virtual testing and evaluation process of highly automated vehicles. *VDI Fahrzeugsicherheit*, 2019, Berlin, Germany.

[3] Köhler A, Prinz F, *et al.* How will we travel autonomously? User needs for interior concepts and requirements towards occupant safety. *28th Aachen Colloquium Automobile and Engine Technology*, 2019, Aachen, Germany.

[4] Eggers A, Putzer M and Kramer S. Investigation of repeatability and reporducibility of the dummy THOR-M in sled and component tests. *crash.tech Conference*, 2016, Munich, Germany.

[5] Edwards M A and Nash C E. Inflatable shoulder belts and inboard upper anchor shoulder belt geometry in far-side oblique impacts. *IRCOBI Conference Proceedings*, 2017, Antwerp, Belgium.

[6] Boin M. Occupant protection in alternative seating positions. *LS-Dyna Forum Conference*, 2018, Bamberg, Germany.

[7] Kitagawa Y, Hayashi S, Yamada K and Gotoh M. Occupant kinematics in simulated autonomous driving vehicle collisions: influence of seating position, direction and angle. *Stapp Car Crash Journal, 2017,* Vol. 61, pp.101-155.

[8] Jin X, Hou H, Shen M, Wu H and Yang K H. Occupant kinematics and biomechanics with rotatable seat in autonomous vehicle collision: A preliminary concept and strategy. *IRCOBI Conference Proceeding*, 2018, Athens, Greece.

[9] Zhao J, Katagiri M, Lee S and Hu J. GHBMC M50-O-Occupant response in a frontal crash of automated vehicle. *Human Modeling and Simulation (carhs) Conference*, 2018, Berlin, Germany.

[10] Dickinson E T. Neck & Neck. Seat belt sign on the neck is as serious a finding as on the abdomen. *Journal of Emergency Medical Service,* 2010, Vol. 34, pp.7-36.

[11] TASS International BV. Model manual, MADYMO Application Model for Integrated Safety (Version 3.0). *TASS International*, Rijswijk, Netherlands, 2018.

[12] Iraeus J. and Lindquist M. Development and validation of a generic finite element vehicle buck model for the analysis of driver rib fracturesin real life nearside oblique frontal crashes. *Accident Analysis & Prevention,* 2016, Vol. 95, pp.42-56.

[13] TASS International BV. Model manual, Active Human Model (Version 3.1). *TASS International*, Rijswijk, Netherlands, 2018.

[14] National Highway Traffic Safety Administration (NHTSA). New car assessment program, Docket No. NHTSA–2006–26555, 11 July, 2008.

VIII. APPENDIX

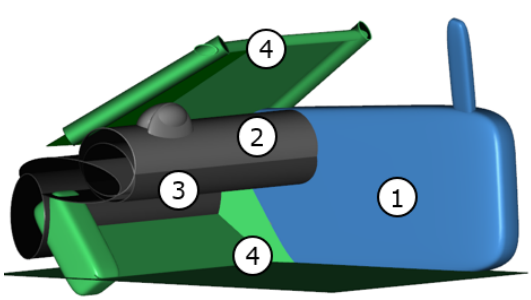

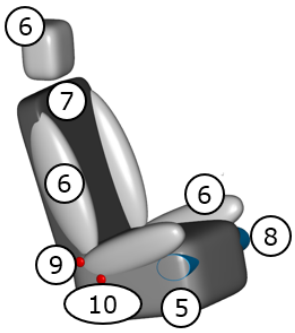

1. Door
2. Instrument Panel (IP)
3. Knee bolster
4. Rigid parts
5. Seat cushion foam
6. Seat bolster and headrest foam
7. Seat backrest foam
8. Anti submarining device
9. Seat recliner
10. Seat tilt

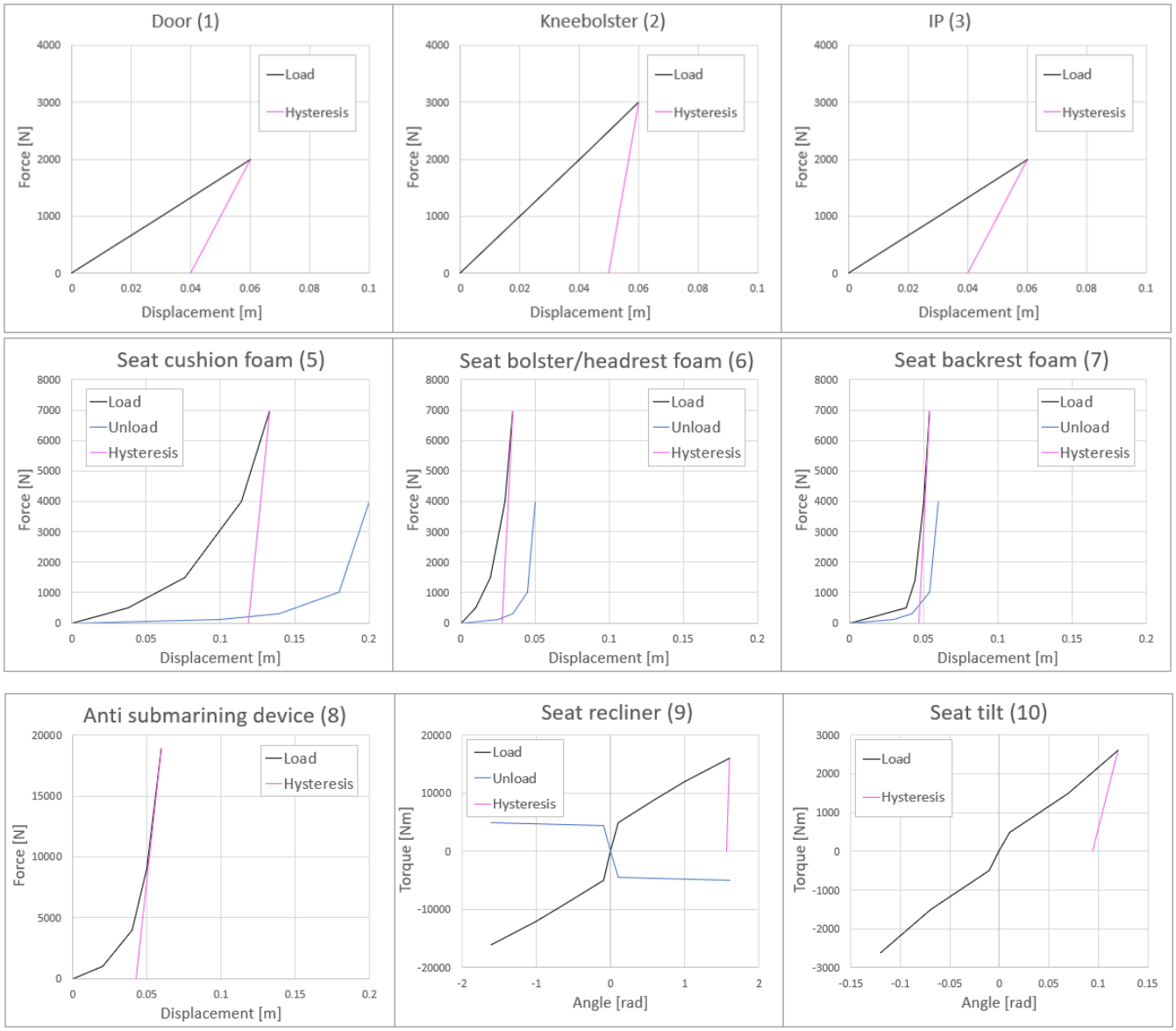

Fig. A1. Vehicle and seat contact characteristics (1-8) and joint restraint characteristics (9-10).

TABLE AI
GENERIC MODEL PARAMETER SETTINGS

	Description	Unit	Value
Load-case parameters	Time step	s	5e-6
	Time-based hands grip release	s	0.0
	Maximum grip force for hands	N	50
	Duration of max grip force for hands	s	0.001
	Time-based wrist and R-U joint unlocking	s	0.0
	Hand grip force threshold for wrist and R-U joint unlocking	N	40
	Duration of hand grip force threshold for wrist and R-U joint unlocking	s	0.001
Seat parameters	Seat Rail Angle w.r.t horizontal	°	10
	Seat Cushion Tilt Angle [deg] w.r.t. Seat Rail	°	4
	Seat Cushion Tilt Stiffness Multiplier	-	1
	Seat Longitudinal Adjustment (forward=-0.1, mid=0.0, rearward=0.1)	m	0.0
	Seat Height Adjustment	m	0
	Seat Back Angle w.r.t vertical	°	-22
	Seat Back Stiffness Multiplier	-	1
	Head Rest X, Z - Position	m	0, 180
	Head Rest Orientation	°	-15
Belt parameters	Acceleration threshold for ball sensor	g	0.45
	Acceleration threshold for webbing pay-out	g	0.3
	Spool stroke (initial length of webbing on spool)	m	0.5
	Elastic limit for film spool effect	m	0.005
	Retractor spool spring pull-in force	N	10
	Belt webbing width (m)	m	0.05
	Belt webbing thickness (m)	m	0.001
	Belt webbing density (kg/m3)	kg/m3	1325
	Belt webbing relative webbing elongation at 11.1 kN pulling force	-	0.102
	Belt elastic limit	m	0.01
	FE belt webbing stiffening factor	-	1
Active Human Model parameters	AHM h-point position ref to Oscar H-point (X, Y, Z)	mm	-3, 0, 7
	AHM orientation in vehicle coordinate system (Z-rotation w.r.t. dummy looking towards vehicle +X-axis)	°	180
	Pelvis pitch up angle - w.r.t. global horizontal plane	°	35.74
	Slouch level (-3.6 = spine stretched to max. / 0.0 = standing erect / 1.0 = normal seated / 6.1 = spine bent to max. (fully slouched))	-	1.0
	Head pitch up angle - w.r.t. global horizontal plane	°	0
	Shoulder (L/R) pitch down angle - w.r.t. arms straight down	°	46
	Elbow (L/R) pitch up angle - w.r.t. arms straightened	°	35
	Upper arm (L/R) torsion angle - lower arm inward when elbow bent	°	45
	Lower arm (L/R) torsion angle - thumbs inward when lower arms forward	°	0
	Wrist (L/R) bending angle - hands inward when lower arms forward with thumbs up	°	-35
	Wrist (L/R) waving angle - hands upward when lower arms forward with thumbs up	°	15
	Hip (L/R) pitch up angle - w.r.t. erect standing posture	°	70.7
	Hip (L/R) adduction angle - upper leg outward rotation	°	0
	Knee (L/R) pitch down angle - w.r.t. erect standing posture	°	59.5
	Ankle (L/R) pitch down angle - w.r.t. erect standing posture	°	5
	Activation parameters for Neck and Spine	-	on
	Activation parameters for Shoulders, Elbows, Hips and Knees	-	off
	Head-Neck reference controller target	-	T1 Body
	Neck co-contraction (None: 0, Full: 1)	-	0.5
	Constant Neck co-contraction 0, variable Neck co-contraction: 1	-	0
	Reaction time	s	0.02
	Delay enable/disable switch (0: no delays, 1: delays)	-	1
	Muscle strength factors	-	1

TABLE AII

ANIMATION OVERVIEW (TOPVIEW)

	PP1 (run_071)	PP1 (run_091)	PP2 (run_071)	PP2 (run_091)
-750 ms	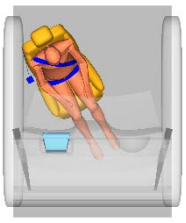		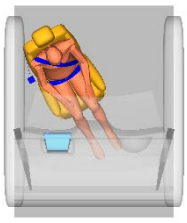	
-500 ms	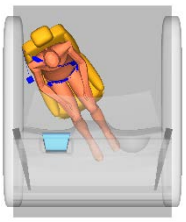	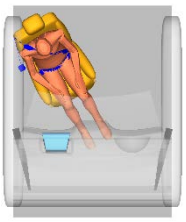	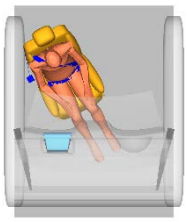	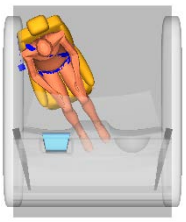
-250 ms				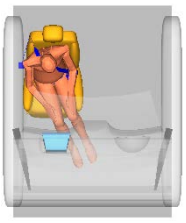
0 ms		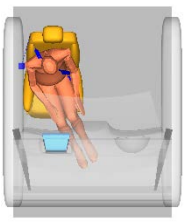	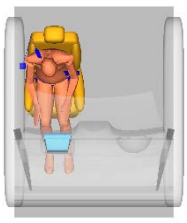	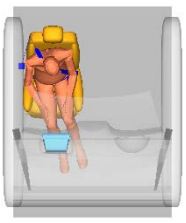
35 ms	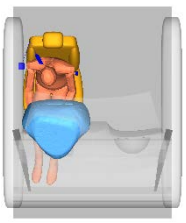		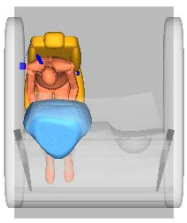	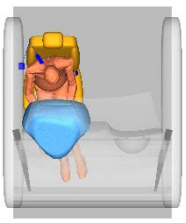
105 ms	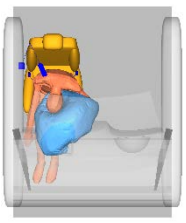	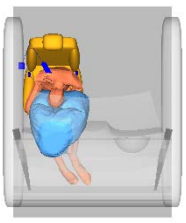	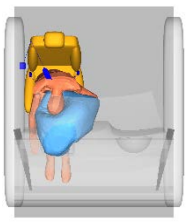	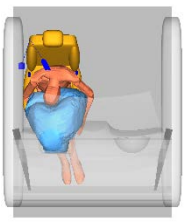
180 ms